



University of Mohamed Khider of Biskra
Faculty of Science and Technology
Department of Mechanical Engineering

Theme submitted for obtaining the degree of

Master

Domain: Sciences and Technology

Sector: Mechanical Engineering

Specialty: Energy

Ref:

Presented and sustained by:

Mr. Mohamed Ouail AOUN

Mr. Abdelatif RAHMANI

On: 28 June 2022

Numerical study of the effect of environmental parameters on the soil surface temperature

The jury members:

Mr. Abdelhafid MOUMMI	Pr	University of Biskra	President
Mr. Abdelouhad ALIOUALI	MCA	University of Biskra	Supervisor
Mr. Chawki MAHBOUB	MCB	University of Biskra	Examiner

University year: 2021-2022



بِسْمِ اللَّهِ الرَّحْمَنِ الرَّحِيمِ

In the name of Allah the most
Gracious and the most Merciful

Dedication

*To my parents, the reason who I am here today
thank you for your great support and continued
care.*

*To my brothers, sisters and all family members,
I am really grateful to you as my inspiration and
friends in my soul.*

*To all of my professors at all educational levels
for your hard work.*

To each of my friends, one by one.

*To my country, who gave me valid
educational opportunities.*

To everyone who participated in this theme

Acknowledgement

*Praise be to **Allah** , first of all, who guided us to this and predestine for us reasons and people*

Then

*Thank you to **my parents**, the reason I am here today for their great support and constant care.*

Thanks to my supervisor, who spared no effort and did not spare us anything despite the difficulties we faced,

Dr. Abdelouahad Aliouali.

*I also thank the kind-hearted **chief of the department**, **Dr. Guerira Belhi**, who provided us with facilities and was close to us throughout our stay in the Mechanical*

Engineering Department, as well as my cousin,

Dr. Yassin AOUN for his continuous guidance

Thanks and all My appreciation to the discussion committee

Pr Abdalhafid MOUMMI and **Dr Chawki MAHBOUB** It was an honor to me that you discussed my memoir. Thanks' to all the **mechanical engineering training team**

Contents

Dedications	
Acknowledgement	
Contents	I
List of Figures	IV
List of Tables	V
Nomenclature	VI
General introduction	1

Chapter I: Literature review

Chapter II: theoretical study

II.1	Introduction	11
II.2	Heat conduction	11
II.3	Heat convection	12
II.3.2	Type of convection	12
II.3.2.a	Natural convection	12
II.3.2.b	Forced convection	12
II.4	Heat radiation	13
II.4.1	Definition	13
II.4.2	Laws of Radiation	14
II.4.2.a	Wien's law	14
II.4.2.b	Kirchhoff's law	14
II.4.2.c	The Stefan-Boltzmann law	14
II.4.3	Shortwave and longwave radiation (R_S-R_L)	14
II.4.3.a	Shortwave radiation (visible light)	14
II.4.3.b	longwave radiation (infrared light)	15
II.5	Thermal Properties of Soil	15
II.5.1	Thermal Conductivity	15

II.5.2	Heat Capacity (C)	16
II.5.3	Thermal Diffusivity	17
II.6	The surface energy balance	17
II.6.1	Net radiation R_n	18
II.6.2	Sensible heat flux H	20
II.6.3	Latent heat flux $L_v E$	20
II.6.3.a	Evaporation – condensation	20
II.7	Conclusion	22
	References	23

Chapter III: Mathematical Modeling And Numerical Simulation

III.1	Introduction	24
III.2	General principles of the finite volume method	24
III.3	Equation of the problem	24
III.4	The boundary conditions	25
III.4.a	Boundary conditions on the top face (soil surface)	25
III.4.b	Boundary conditions on the bottom face (subsoil)	25
III.4.c	Boundary condition on the frontier (right left)	26
III.5	Domain discretization	26
III.6	Discretization of the equation	27
III.7	Solution of Algebraic Equations	28
III.7.1	Thomas algorithm or the TDMA (TriDiagonal-Matrix Algorithm).	28
III.7.2	Summary of the algorithm	30
III.8	Simulation part	31
III.8.1	Station description.	31
III.8.2	Meteorological data	32
III.8.3	Calculating Algorithms	33
III.9	Conclusion.	35
	References	36

Chapter IV:Resulte And discussion

IV.1	Introduction	37
IV.2.a	Effect of solar radiation	37
IV.2.b	Effect of ambient temperature	38
IV.2.c	Effect of Wind speed	39
IV.2.d	Effect of relative humidity	40
IV.2.e	Effect of fractional cloud cover coefficient	40
IV.2.f	Effect of surface Albedo	41
IV.2.g	Effect of surface emissivity	42
IV.3	Conclusion	43
	General conclusion	44

List of Figures

Figure II.1	Heat conduction through a wall.	11
Figure II.2	Convection heat transfer processes.(a) Forced convection.(b) Natural convection. (c) Boiling. (d) Condensation	13
Figure II.3	Radiation exchange,(a) at a surface	14
Figure II.4	Surface energy balance	17
Figure III.1	Soil modeling	25
Figure III.2	Calculation mesh	26
Figure III.3	Control volume	26
Figure III.4	Scheme of Algorithm for calculating for an average monthly day	33
Figure III.5	Scheme of Algorithm for calculating surface temperature for 24 hours . . .	34
Figure IV.1	Evolution of surface temperature for different solar radiation values over 24h	37
Figure IV.2	Evolution of surface temperature for different ambient temperature values over 24h. .	38
Figure IV.3	Evolution of surface temperature for different wind speed values over 24h. .	39
Figure IV.4	Evolution of surface temperature for different relative humidity values over 24	40
Figure IV.5	Evolution of surface temperature for different cloud number values over 24h	41
Figure IV.6	Evolution of surface temperature for different Albedo values during 24h . .	42
Figure IV.7	Evolution of surface temperature for different emissivity values during 24h.	43

List of Tables

TABLE II.1	Thermal conductivity, density, and specific heat of common soil constituents at 10 °C.	16
TABLE II.2	Basic Empirical Methods to Estimate Atmospheric Emissivity.	19
TABLE III.1	The proprieties of the soil in the region of Biskra.	31
TABLE III.2	Annual ambient meteorological data (meteorological station of Biskra, 2005).	32

Nomenclature

Glossary:

A	Surface area of heat flow(perpendicular to the direction of flow)	m^2
T_{soil}	Soil surface temperature	K
T_{air}	Air temperature	K
T_a	Air Temperature at 2 m Height	K
R_n	The net radiation	W/m^2
R_{ns}	The incoming net shortwave radiation	W/m^2
R_{nL}	The outgoing net longwave radiation	W/m^2
R_{s↓}	The surface incident solar radiation (direct and diffuse)	W/m^2
R_{s↑}	The surface reflected solar radiation (shot wave)	W/m^2
R_{L↓}	The atmospheric downward longwave radiation	W/m^2
R_{L↑}	The surface emitted longwave radiation	W/m^2
G	The heat storage in the ground	W/m^2
Q	Heat flow through a body	Watts
dt	Temperature difference of the faces of block,	K
dx	Thickness of body in the direction of flow	m
k	Thermal conductivity of the body	$W/m \cdot ^\circ k$
C	Volumetric heat capacity	$j/m^3 \cdot k^\circ$
C_p	Specific heat	$j/kg \cdot k$
c_s	The specific heat of the soil solids	$Jg^{-1}C^{-1}$
c_w	The specific heat of water	$Jg^{-1}C^{-1}$
H	The sensible heat flux	W/m^2
h_{conv}	Convective transfer coefficient	$W/m^2 \cdot ^\circ k$
V_{wind}	Wind speed	m/s
L_vE	The latent heat flux	W/m^2
L_v	Latent heat of vaporization of water	J/kg

E	Mass flux of water vapor	kg/s. m²
K_E	Mass transfer coefficient	m/s
M_w	Molar mass of water vapor	kg/mol
R	Ideal gas constant	J/mol.K
RH	Relative humidity.	%
T	Temperature at a point on the ground	K
t	instant of time	s
(x, y, z)	Spatial coordinates of the considered point in the ground	m
T_c	constant temperature at depth	K
e_a	Water Vapor Pressure	hpa

Greek Letters:

α	Soil thermal diffusivity	m²/ s
σ	Stefan-Boltzmann constant	W/m² K⁴
θ	Volumetric water content	cm³ cm⁻³
ρ	Density	kg/ m³
ρ_b	The soil bulk density	g/ m³
ρ_w	The density of water	g/ m³
λ	Average thermal conductivity of soil	W/m K

Non dimensional Letters

α	The albedo at the surface
λ_m	The emissive power of a black body
ε_{atm}	the emissivity of the atmosphere
ε_{sol}	emissivity of the soil (non dimensional)
C_{cloud}	The fraction cloud cover coefficient

Abbreviations:

CFD: Computational Fluid Dynamic

FVM: Finite volume method

LTGE: low temperature geothermal energy

MATLAB: MATrix LABoratory

TDMA: Tri Diagonal-Matrix Algorithhm

*General
Introduction*

General Introduction:

Soil temperature play the key role in the design of low temperature geothermal energy (LTGE) systems. LTGE is increasingly utilized nowadays in heating and cooling applications in order to reduce dependence on fossil fuels, and as a tool to control earth global warming. It also influences the interspheric processes of gas exchange between the atmosphere and the soil (Lehnert, 2014). Soil temperature is one of the important factors that influence soil properties involved in plant growth. It governs the soil physical, chemical and biological processes (Buchan, 2001). The temperature of the soil alters the rate of organic matter decomposition and the mineralization of different organic materials in the soil (Davidson and Janssens, 2006). Soil temperature also affects soil water retention, transmission and availability to plants.

According to studies, the heat flow within the ground is affected by several factors, such as solar radiation, wind speed, days of the year, soil properties and so on.

Due to its importance and the severity of its need and the lack of information on it, it is therefore necessary for us to interest and contribute to improving knowledge of the phenomena related to it and how the environmental factors affect the soil's surface temperature.

In the **first chapter** we'll present some of the works that were previously studied in the same field to determine the location of our work and categorize it among the previous works.

The **second** chapter we'll present the transport processes of heat within the soil and exchange of heat between the soil and the atmosphere. It based on theoretical study of surface energy balance. This study used to put equation that predict the variations of soil surface temperature.

In the **third chapter**, we'll solve the energy balance equation that we extracted on the precedent chapter, present the method (FVM) and the different parameters that aide us step by step.

The **final chapter** will present the data and discuss the results obtained.

Chapter 1

Literature review

1.1.INTRODUCTION:

In order to determine the location of our work and categorize it among the previous works, we try in this chapter to present some of the works that were previously studied in the same field.

1.2.Previously studied works:

Among the works that have been studied and related to our work are summarized as follows:

G. Mihalakakou et al. (1992) [1].

On the application of the energy balance equation to predict ground temperature profiles

They have developed simple and accurate models for predicting the annual variation of ground temperature at the Earth's surface and at different depths. Algorithms for predicting the daily variation at the ground surface are also proposed. Finally, the results of the global analysis are compared with corresponding data from other known measurement sets. Global analysis is useful for predicting the performance of buildings in direct contact with the ground as well as for the performance of the efficiency of ground-to-air heat exchangers.

G. Mihalakakou et al. (1994) [2].

Measurements of ground temperature at various depths

Presented a new comprehensive numerical model for the prediction of the thermal performance of earth-to-air heat exchangers. The model describes the simultaneous heat and mass transfer inside the tube and in the ground, taking into account the natural thermal stratification of the ground. The model is validated against a large set of experimental data and found to be accurate. The proposed algorithms are suitable for calculating the variation of temperature and humidity of circulating air and for the distribution of temperature and humidity in soil.

G. Mihalakakou et Al (1997) [3].

Simple and accurate model for the ground heat exchanger of passive house

Used a comprehensive model for the prediction of daily and annual soil temperature variation. This model is based on the differential equation with transient thermal conduction using as boundary condition the equation of the energy balance at the surface of the ground. The energy balance equation involves the exchange of energy by convection between the air and the ground; solar radiation absorbed by the ground surface, latent heat flux due to evaporation at the ground surface as well as long wave radiation. A sensitivity study was performed to assess the impact of various factors involved in the ground surface energy balance equation on the ground temperature

distribution. The global analysis is useful for the prediction of the thermal performance of buildings in direct contact with the ground as well as for the prediction of the energy efficiency of ground-air heat exchangers.

Sedlak P. (1998) [4].

Retrieving soil temperature profile by assimilating MODIS LST products with ensemble Kalman filter

Studied the influence of surface roughness, geotropic wind speed and from stable initial stratification to superficial layer scales.

Best M. J. (1998) [5].

Soil Temperature Estimation by a Numerical Method

Described a model for predicting the surface temperature of a variety of surfaces. The model solves the surface energy balance equation iteratively, using only standard meteorological data. It has been shown that, to obtain the rates of correct cooling of the vegetation during the night, it was necessary to subtract the direct influence of the flow of the soil to the equation of the energy balance of the vegetation layer. A diagram coupling a cover ground plant only by radiation is described, giving cooling rates satisfactory with respect to observations..

KANG, Sinkyu et al 2000 [6].

Predicting spatial and temporal patterns of soil temperature based on topography, surface cover and air temperature.

They was developed in this study, a hybrid soil temperature model to predict daily spatial patterns of soil temperature in a forested landscape by incorporating the effects of topography, canopy and ground litter. The model is based on both heat transfer physics and empirical relationship between air and soil temperature, and uses input variables that are extracted from a digital elevation model (DEM), satellite imagery, and standard weather records. Model-predicted soil temperatures fitted well with data measured at 10 cm soil depth at three sites: two hardwood forests and a bare soil area. A sensitivity analysis showed that the model was highly sensitive to leaf area index (LAI) and air temperature. When the spatial pattern of soil temperature in a forested watershed was simulated by the model, different responses of bare and canopy-closed ground to air temperature were identified. Spatial distribution of daily air temperature was geostatistically interpolated from the data of weather stations adjacent to the simulated area. Spatial distribution of LAI was obtained from Landsat Thematic Mapper images. The hybrid model describes spatial variability of soil temperature across landscapes and different sensitivity to rising air temperature depending on site-

specific surface structures, such as LAI and ground litter stores. In addition, the model may be beneficially incorporated into other ecosystem models requiring soil temperature as one of the input variables.

G.Mhalakakou 2002 [7].

On estimating soil surface temperature profiles.

This study presented two methods for modeling and estimating the daily and annual variation of soil surface temperature. Soil surface temperature is an important factor for calculating the thermal performance of buildings in direct contact with the soil as well as for predicting the efficiency of earth-to-air heat exchangers. The two estimation methods are a deterministic model and a neural network approach. The two methods are tested and validated against extensive sets of measurements for bare and short-grass covered soil in Athens and Dublin. Finally, the comparison of the two models showed that the proposed intelligent technique is able to adequately estimate the soil surface temperature distribution.

Richard Allen et al 2002 [8].

SEBAL (surface energy balance algorithms for land).

This study explains a remote image-processing model for predicting evapotranspiration ET termed SEBAL (Surface Energy Balance Algorithm for Land). SEBAL calculates evapotranspiration ET through a series of computations that generate: net surface radiation, soil heat flux, and sensible heat flux to the air. By subtracting the soil heat flux and sensible heat flux from the net radiation at the surface we are left with a “residual” energy flux that is used for evapotranspiration (i.e. energy that is used to convert the liquid water into water vapor). This manual describes the theoretical basis of SEBAL using images from Landsat 5 and 7 satellites. However, the theory is independent of the satellite type and this manual could be applied to other satellite images if used with appropriate coefficients.

XIA Zhang 2010 [9].

Simulation of the Bare Soil Surface Energy Balance at the Tongyu Reference Site in Semiarid Area of North China.

They studied the performance of a 1-D soil model in a semiarid area of North China was investigated using observational data from a cropland station at the Tongyu reference site of the Coordinated Enhanced Observing Period (CEOP) during the non-growing period, when the ground surface was covered with bare soil. Comparisons between simulated and observed soil surface energy balance components as well as soil temperatures and water contents were conducted to

validate the soil model. Results show that the soil model could produce good simulations of soil surface temperature, net radiation flux, and sensible heat flux against observed values with the RMSE 2–C, 7.71 W m² of 1.54 2–, and 27.79 W m², respectively. The simulated volumetric soil water content is close to the observed values at various depths with the maximal difference between them being 0.03. Simulated latent heat and ground heat fluxes have relatively larger errors in relative to net radiation and sensible heat flux. In conclusion, the soil model has good capacity to simulate the bare soil surface energy balance at the Tongyu cropland station and needs to be further tested in longer period and at more sites in semiarid areas

Irvine, Peter J et al 2011 [10].

Climatic effects of surface albedo geoengineering

In this study present results of a series of atmosphere–ocean general circulation model (GCM) simulations to compare three surface albedo geoengineering proposals: urban, cropland, and desert Albedo enhancement. We find that the cooling effect of surface albedo modification is strongly seasonal and mostly confined to the areas of application. For urban and cropland geoengineering, the global effects are minor but, because of being collocated with areas of human activity, they may provide some regional benefits. Global desert geoengineering, which is associated with significant global-scale changes in circulation and the hydrological cycle, causes a smaller reduction in global precipitation per degree of cooling than sunshade geoengineering, 1.1% K₁ and 2.0% K₁ respectively, but a far greater reduction in the precipitation over land, 3.9% K₁ compared with 1.0% K₁. Desert geoengineering also causes large regional-scale changes in precipitation with a large reduction in the intensity of the Indian and African monsoons in particular. None of the schemes studied reverse the climate changes associated with a doubling of CO₂, with desert geoengineering profoundly altering the climate and with urban and cropland geoengineering providing only some regional amelioration at most.

Bicalho. K.V and al 2013 [11].

Study of the influence of climatic effects on the soil temperature and suction changes.

In this study, they focused on predicting of temperature and suction response to climatic changes in a soil profile during a long-term period by considering the soil atmosphere interface interactions, with emphasis on evaporation. A one-dimensional model is used to calculate the evaporation rate and heat flux on the soil surface; water (liquid and vapor) transport equations coupled to heat flow

equation are solved to determine the soil profiles. The investigated site, in France, has been instrumented with a meteorological station in order to monitor solar radiation, precipitation, wind speed, air temperature, and air relative humidity. A water deficit is observed in most of time throughout the instrumented years. The results show that the active zone is about 1.5 m deep in the investigated region and the actual monitored meteorological data, and would fluctuate 3 m by using the average data. Calculated and direct measurements were compared and satisfactory results were obtained.

Mabrouki Djamel 2013 [12].

Étude de l'influence des paramètres climatiques sur la température du sol (application au site de Biskra).

This work relates to the study of the influence of climatic and environmental parameters as well as their influence on soil temperature. Through numerical modeling, followed by a computer code, we have shown the evolution of the temperature of the ground surface as well as the different heat fluxes exchanged between the ground and the surrounding environment. Finally they gave the results of an experimental study relating to a Canadian well installed at the University of Biskra.

Aicha BENMECHETA 2016 [13].

Estimation de la température de surface à partir de l'imagerie satellitale; validation sur une zone côtière d'Algérie

the main objective in this work is two-pronged the first one to present a review of the main surface temperature T_s extraction methods, highlighting their algorithmic particularities, respective parameters, and constraints, and the seconde one to develop an extraction and processing tool for the surface temperature and its use for the monitoring of the landscape evolution. The algorithms discussed in this thesis employ a number of methods to calculate the surface temperature based on satellite data; the interface allows a user-friendly selection of the most suitable extraction method for the user's study. This work is accomplished using IDL programming language.

Shweta Sharma et al 2017 [14].

Effect of urban surface albedo enhancement in India on regional climate cooling.

They studied in this work, the impact of surface albedo change (by using white paint on roofs in India) on radiative forcing and land surface temperature change has been quantified based on the principles of Physics using energy balance equation and one-layer atmospheric model. The reduction in temperature from enhanced surface albedo was related to the offsets in temperature increase due to carbon dioxide concentration change from pre-industrial to present times. For Indian region, land surface temperature was found to decrease by $\sim 0.63 \pm 0.04$ K considering water vapour feedback effect and total outgoing radiation increased by $\sim 1.314 \text{ W/m}^2$, for an increase in area weighted surface albedo by 0.0037. The effect of urban albedo enhancement on the land surface temperature change was simulated and it was found to be in the range of -1 to $+1$ K with the mean value of -0.043 K. Radiative forcing due to Carbon dioxide concentration change from pre-industrial to present times was calculated as 1.797 W/m^2 and corresponding land surface temperature change estimated was ≈ 0.86 K. The study concluded that use of cool roofs in India can compensate the heating due to increase in CO_2 concentration (from pre-industrial times to present times) by $\sim 5\%$.

Brownmang onwuka et al 2018 [15].

Effects of soil temperature on some soil properties and plant growth

Soil temperature varies seasonally and daily which may result from changes in radiant energy and energy changes taking place through the soil surface. It governs the soil physiochemical and biological processes and also influences the interspheric processes of gas exchange between the atmosphere and the soil. Environmental factors affect soil temperature by either controlling the amount of heat supplied to the soil surface and the amount of heat dissipated from the soil surface down the profile. Soil temperature alters the rate of organic matter decomposition and mineralization of different organic materials. It also affects soil water content, its conductivity and availability to plants. The paper introduced soil temperature as a major determinant of the processes that takes place in the soil which are necessary for plant growth.

Faridi Hamide et al 2019 [16].

Utilization of Soil Temperature Modeling to Check the Possibility of Earth-Air Heat Exchanger for Agricultural Building.

In this research, they studied the thermal potential of the soil profile in Kouhsar, Alborz province, Iran, for utilizing the shallow geothermal energy in order to supply thermal demands of building like greenhouses. Therefore, the temperature sensors were set at the four depths of 30, 100, 200, and 300 cm as well as at the ground surface. The results showed that the greater the depth, the less fluctuation of the soil temperature as well as the greater the temperature difference of the soil profile against the ambient air temperature. These results suggest that the potential of the earth could be used to warm up or cool down in this location for an agricultural structure like greenhouse. The soil profile temperature behavior was modeled at different depths by two methods as heat transfer and empirical. The empirical model was simpler than the other one. As the possibility of using geothermal energy in this region has not been investigated.

Angelini Lucas Peres and al 2021 [17].

Surface Albedo and Temperature Models for Surface Energy Balance Fluxes and Evapotranspiration Using SEBAL and Landsat 8 over Cerrado-Pantanal, Brazil.

The objective of this study is to evaluate the performance of algorithms used to calculate surface albedo and surface temperature on the estimation of SEBFs and ET in the Cerrado-Pantanal transition region of Mato Grosso, Brazil. Surface reflectance images of the Operational Land Imager (OLI) and brightness temperature (T_b) of the Thermal Infrared Sensor (TIRS) of the Landsat 8, and surface reflectance images of the MODIS MOD09A1 product from 2013 to 2016 were combined to estimate SEBF and ET by the surface energy balance algorithm for land (SEBAL), which were validated with measurements from two flux towers. The surface temperature (T_s) was recovered by different models from the T_b and by parameters calculated in the atmospheric correction parameter calculator (ATMCORR). A model of surface albedo (a_{sup}) with surface reflectance OLI Landsat 8 developed in this study performed better than the conventional model (a_{con}) SEBFs and ET in the Cerrado-Pantanal transition region estimated with as up combined with T_s and T_b performed better than estimates with a_{con} . Among all the evaluated combinations, SEBAL performed better when combining a_{sup} with the model developed in this study and the surface temperature recovered by the Barsi model ($T_{S_{baris}}$).

References :

- [1] **G. Mihalakakou, M. Santamouris, J.O. Lewis and D.N. Asimakopoulis** “On the application of the energy balance equation to predict ground temperature profiles” *Solar energy* V60, 1997, pp 181-190.
- [2] **F. Georgios and K. Soteris** “Measurements of ground temperature at various depths” Techniques paper of Higher Technical Institute Nicosia Cyprus 2005.
- [3] **ViorelBadescu** “Simple and accurate model for the ground heat exchanger of passive house” *Renewable energy* 32, 2007; pp 845-855.
- [4] **Chunlin Huang, Xin Li, Ling Lu** “Retrieving soil temperature profile by assimilating MODIS LST products with ensemble Kalman filter” *Remote Sensing of Environment* 112 (2008) pp 1320–1336
- [5] **R. J. Hanks, D. D. Austin and W. T. Ondrechen** “Soil Temperature Estimation by a Numerical Method” *Soil Science Society of America Journal* Vol. 35 No. 5, p. 665-667
- [6] **KANG, Sinkyu, et al.** Predicting spatial and temporal patterns of soil temperature based on topography, surface cover and air temperature. *Forest Ecology and Management*, 2000, 136.1-3: 173-184.
- [7] **MIHALAKAKOU, G.** On estimating soil surface temperature profiles. *Energy and Buildings*, 2002, 34.3: 251-259.
- [8] **ALLEN, R. G., et al.** SEBAL (surface energy balance algorithms for land). *Advance training and users manual–Idaho implementation, version*, 2002, 1: 97.
- [9] **XIA, Zhang.** Simulation of the bare soil surface energy balance at the Tongyu reference site in semiarid area of north China. *Atmospheric and Oceanic Science Letters*, 2010, 3.6: 330-335.
- [10] **IRVINE, Peter J.; RIDGWELL, Andy; LUNT, Daniel J.** Climatic effects of surface albedo geoengineering. *Journal of Geophysical Research: Atmospheres*, 2011, 116.D24.
- [11] **BICALHO, K. V.; VIVACQUA, G. P. W.; CUI, Y. J.** Study of the influence of climatic effects on the soil temperature and suction changes. 2013.
- [12] **MABROUKI, Djamel.** *Étude de l'influence des paramètres climatiques sur la température du sol (application au site de Biskra)*. Master Thème. Université Biskra. 2013.
- [13] **BENMECHETA, Aicha.** *Estimation de la température de surface a partir de l'imagerie satellitale; validation sur une zone côtière d'Algérie*. 2016. PhD Thesis. Université Paris-Est.
- [14] **SHARMA, Shweta, et al.** Effect of urban surface albedo enhancement in India on regional climate cooling. *Remote Sensing Applications: Society And Environment*, 2017, 8: 193-198.

[15] Onwuka, Brownmang, and B. Mang. "Effects of soil temperature on some soil properties and plant growth." *Adv. Plants Agric. Res* 8.1 (2018): 34

[16] FARIDI, Hamideh, et al. Utilization of Soil Temperature Modeling to Check the Possibility of Earth-Air Heat Exchanger for Agricultural Building. *Iranian (Iranica) Journal of Energy & Environment*, 2019, 10.4: 260-268.

[17] ANGELINI, Lucas Peres, et al. Surface Albedo and Temperature Models for Surface Energy Balance Fluxes and Evapotranspiration Using SEBAL and Landsat 8 over Cerrado-Pantanal, Brazil. *Sensors*, 2021, 21.21: 7196.

Chapter II

Theoretical Study

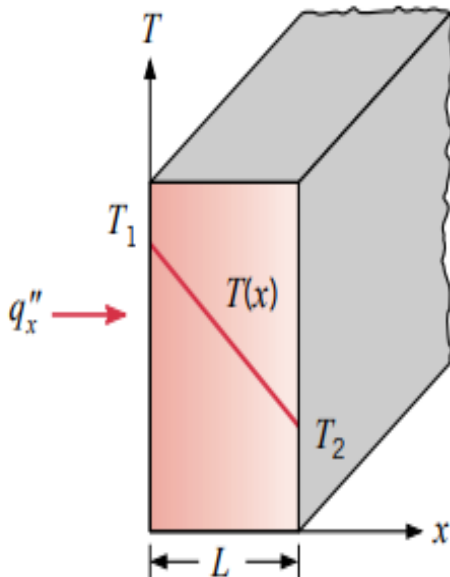
II.1.Introduction:

Soil temperatures are determined by the transport processes of heat within the soil and exchange of heat between the soil and the atmosphere as the surface energy balance . There are three different processes where by heat can be transported conduction, convection, and radiation.

II.2.Heat Conduction:

Conduction is heat transfer by means of molecular agitation within a material without any motion of the material as a whole. If one end of a metal rod is at a higher temperature, then energy will be transferred down the rod toward the colder end because the higher speed particles will collide with the slower ones with a net transfer of energy to the slower ones [1].

Fourier’s law of heat conduction is an empirical law based on observation and states as follows : “The rate of flow of heat through a simple homogeneous solid is directly proportional to the area of the section at right angles to the direction of heat flow, and to change of temperature with respect to the length of the path of the heat flow”.



Mathematically, it can be represented by the equation:

$$Q \propto A \cdot \frac{dt}{dx} \text{ where,}$$

Q = Heat flow through a body per unit time (in watts),

A = Surface area of heat flow(perpendicular to the direction of flow), m^2

dt =Temperature difference of the faces of block (homogeneous solid) of thickness ' dx ' through which heat flows, $^{\circ}C$ or K , and

dx = Thickness of body in the direction of flow, m

FigureII.1: Heat conduction through a wall [3]

Thus,
$$Q = -k \cdot A \cdot \frac{dt}{dx} \quad (II.1)$$

where, k = Constant of proportionality and is known as thermal conductivity of the body.

The -ve sign of k is to take care of the decreasing temperature along with the direction of increasing thickness or the direction of heat flow. The temperature gradient dt is always negative along positive x direction and, therefore, the value as Q becomes +ve [2].

II.3.Heat Convection:

II.3.1.Definition

Convection is the process of heat transfer by the movement of molecules within fluids such as gases and liquids-the actual motion of matter-. The initial heat transfer between the object and the fluid takes place through conduction, but the bulk heat transfer happens due to the motion of the fluid.

When a fluid is heated from below, thermal expansion takes place. The lower layers of the fluid, which are hotter, become less dense. Due to buoyancy, the less dense, hotter part of the fluid rises up. And the colder, denser fluid replaces it. This process is repeated when this part also gets heated and rises up to be replaced by the colder upper layer.

II.3.2.Type of convection: There are two types of convection, and they are:

II.3.2.a.Natural convection: When convection takes place due to buoyant force as there is a difference in densities caused by the difference in temperatures it is known as natural convection.

II.3.2.b.Forced convection: When external sources such as fans and pumps are used for creating induced convection, it is known as forced convection.[4]

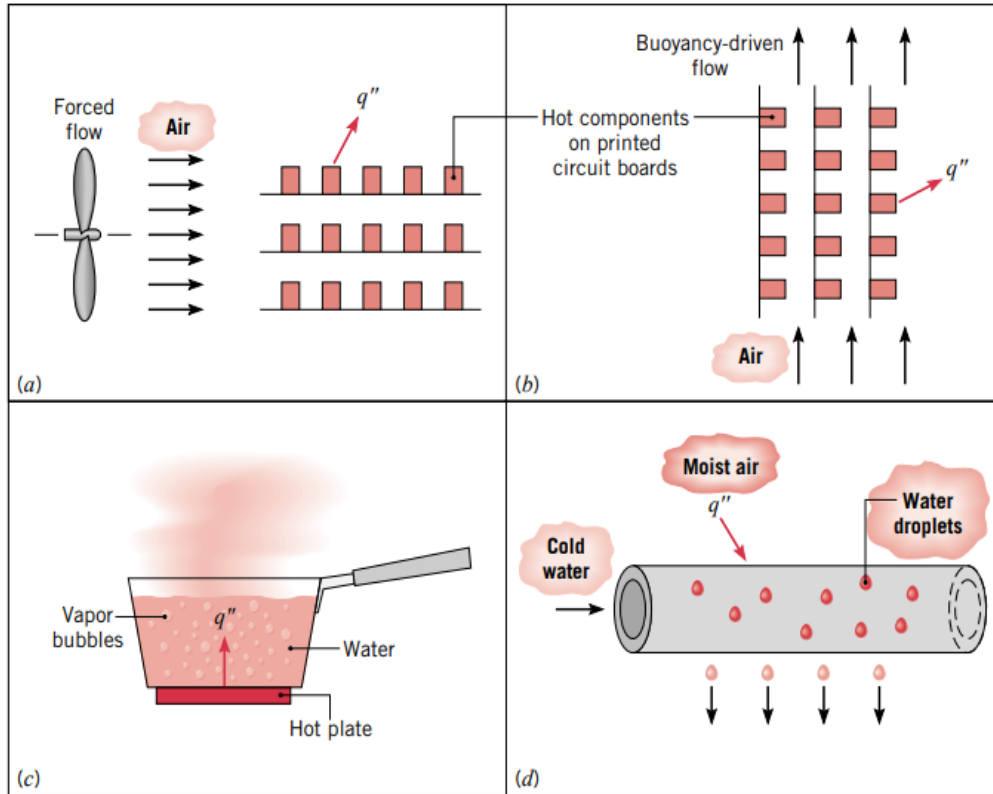


Figure II.2. Convection heat transfer processes. (a) Forced convection. (b) Natural convection. (c) Boiling. (d) Condensation [3].

II.4.Heat radiation:

II.4.1.Definition

Thermal radiation, process by which energy, in the form of electromagnetic radiation, is emitted by a heated surface in all directions and travels directly to its point of absorption at the speed of light; thermal radiation does not require an intervening medium to carry it.

Thermal radiation ranges in wavelength from the longest infrared rays through the visible-light spectrum to the shortest ultraviolet rays. The intensity and distribution of radiant energy within this range is governed by the temperature of the emitting surface. The total radiant heat energy emitted by a surface is proportional to the fourth power of its absolute temperature (the Stefan–Boltzmann law).[5]

II.4.2.Laws of Radiation :

II.4.2.a.Wien’s law: It states that the wavelength X, corresponding to the maximum energy is inversely proportional to the absolute temperature T of the hot body.

$$\lambda_m \propto \frac{1}{T} \quad \text{or} \quad \lambda_m T = \text{constant}$$

II.4.2.b.Kirchhoff’s law: It states that the emissivity of the body at a particular temperature is numerically equal to its absorptivity for radiant energy from body at the same temperature.

II.4.2.c.The Stefan-Boltzmann law: The law states that the emissive power of a black body is directly proportional to fourth power of its absolute temperature.

$$\lambda_m \propto T^4$$

$$Q = F\sigma A. (T_1^4 - T_2^4) \tag{II.2}$$

Where, **F**= A factor depending on geometry and surface properties,

F=1 for a simple cases of black surface enclosed by other surface

F= emissivity (ε) for non-black surface enclosed by other surface

[Emissivity (ε) is defined as the ratio of heat radiated by surface to that of an ideal surface]

σ= Stefan-Boltzmann constant = 5.67 × 10⁻⁸ W/m² K⁴

A= area m² and T₁ , T₂= Temperatures degrees Kelvin (K)

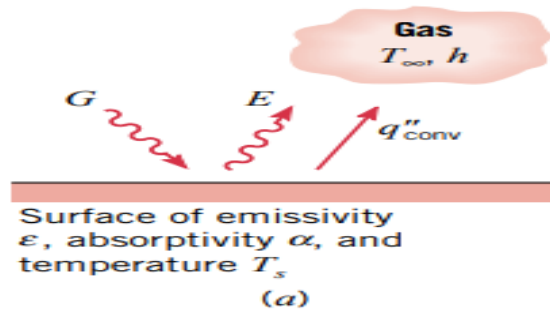


Figure:II.3.Radiation exchange,(a) at a surface[3]

II.4.3. Shortwave and longwave radiation (R_S-R_L)

II.4.3.a.Shortwave radiation (visible light): contains a lot of energy is referred to total solar irradiance with wavelengths in the range of (0.3-3.0 μm);

II.4.3.b.longwave radiation (infrared light): contains less energy than shortwave radiation (shortwave radiation has a shorter wavelength than longwave radiation).

Solar energy enters our atmosphere as shortwave radiation in the form of ultraviolet (UV) rays (the ones that give us sunburn) and visible light. The sun emits shortwave radiation because it is extremely hot and has a lot of energy to give off.[6]

II.5. Thermal Properties of Soil:

The soil thermal properties is necessary to predict how soil temperatures vary in space and time. The primary thermal properties of soil, or any substance, are the heat capacity and the thermal conductivity. The heat capacity can be defined per unit mass, in which case it is often called the specific heat, or per unit volume, in which case it is called the volumetric heat capacity. Sometimes it is useful to consider the ratio of the thermal conductivity to the volumetric heat capacity, and this ratio is called the **thermal diffusivity**.

II.5.1.Thermal Conductivity:

The soil thermal conductivity (λ) is the ratio of the amount of the conductive heat flux through the soil to the amount of the temperature gradient ($W/m.k^\circ$). It is a measure of the soil's ability to conduct heat, just as the hydraulic conductivity is a measure of the soil's ability to "conduct" water. Soil thermal conductivity is influenced by a wide range of soil characteristics including:

- **air-filled porosity**
- **water content**
- **bulk density**
- **texture**
- **mineralogy**
- **organic matter content**
- **soil structure**
- **soil temperature**

Among common soil constituents, quartz has by far the highest thermal conductivity and air has by far the lowest thermal conductivity . Often, the majority of the sand-sized fraction in soils is composed primarily of quartz, thus sandy soils have higher thermal conductivity values than other soils, all other things being equal.

The higher the air-filled porosity is, the lower the thermal conductivity is. Soil thermal conductivity increases as water content increases, but not in a purely linear fashion.

For dry soil, relatively small increases in the water content can substantially increase the thermal contact between mineral particles because the water adheres to the particles, resulting in a relatively large increase in the thermal conductivity.

Table :II.1. Thermal conductivity, density, and specific heat of common soil constituents at 10 °C [7]

Soil constituent	Thermal conductivity $W/m.k^{\circ}$	Density Kg/m^3	Specific heat $J/Kg.k^{\circ}$
Quartz	8.8	2660	750
Clay mineral	3.0	2630	760
Soil organic mater	0.3	1300	1900
Water	0.57	1000	4180
Ice	2.2	920	2000
Air	0.025	1.25	1000

II.5.2.Heat Capacity (C):

Soil *volumetric heat capacity* (C) is the amount of energy required to raise the temperature of a unit volume of soil by one degree ($J/m^3.k^{\circ}$). Unlike thermal conductivity, volumetric heat capacity increases strictly linearly as soil water content increases. Volumetric heat capacity is also a linear function of bulk density. The volumetric heat capacity can be calculated by:

$$C = \rho_b c_s + \rho_w c_w \theta \quad (II.3)$$

where ρ_b is the soil bulk density (g/m^3), c_s is the specific heat of the soil solids ($Jg^{-1}C^{-1}$), ρ_w is the density of water (g/m^3), c_w is the specific heat of water, and θ is the volumetric water content ($cm^3 cm^{-3}$).

To increase the temperature of wetter, denser soil requires more energy than to increase the temperature of drier, less dense soil, which has a lower volumetric heat capacity. This is one

factor that can contribute to lower soil temperatures and delayed crop development in soils managed with no tillage.

II.5.3. Thermal Diffusivity:

The soil *thermal diffusivity* is the ratio of the thermal conductivity to the volumetric heat capacity (m^2/s). It is an indicator of the rate of at which a temperature change will be transmitted through the soil by conduction. When the thermal diffusivity is high, temperature changes are transmitted rapidly through the soil. Logically, soil thermal diffusivity is influenced by all the factors which influence thermal conductivity and heat capacity. Thermal diffusivity is somewhat less sensitive to soil water content than are thermal conductivity and volumetric heat capacity.[7]

II.6. The surface energy balance:

Surface temperatures are controlled locally by a surface energy balance, i.e., the balance between net radiation at the surface and turbulent fluxes of heat, sensible heat flux, latent heat flux and conduction heat flux. These terms have large geographical, seasonal, and (over land) diurnal variations.

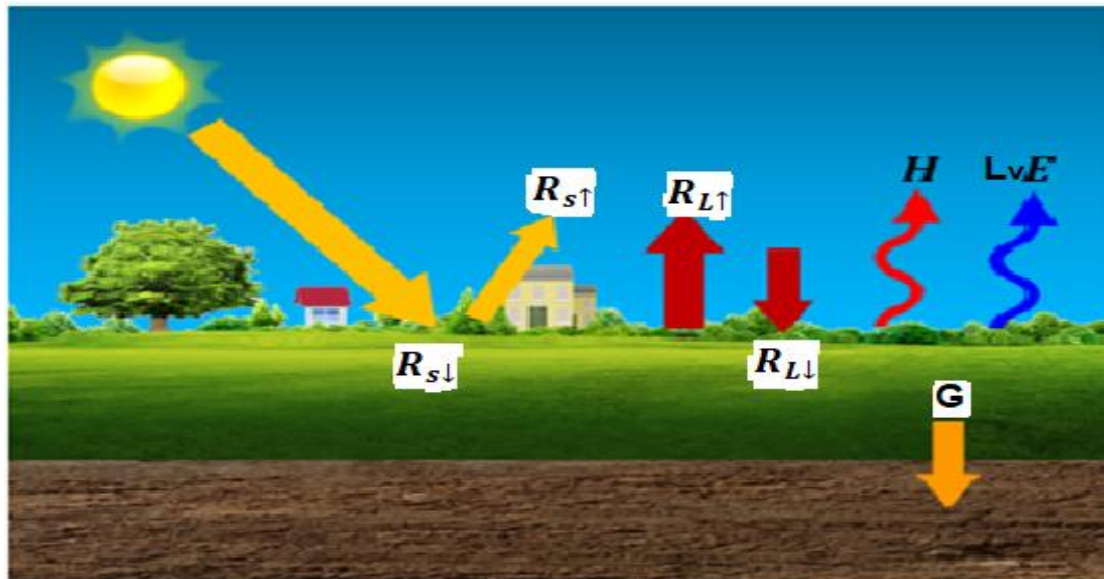


Figure:II.4.surface energy balance [10]

Where

$$R_n = R_{s\downarrow} - R_{s\uparrow} + R_{L\downarrow} - R_{L\uparrow} = L_v E + H + G \quad (II.4)$$

R_n the net radiation W/m^2

$L_v E$ the latent heat flux W/m^2

H the sensible heat flux W/m^2

G the heat storage in the ground W/m^2

Detailed expressions of exchange flows are as follows:

II.6.1. Net radiation R_n :

The net radiation R_n is the difference between the incoming net shortwave radiation R_{ns} and the outgoing net longwave radiation R_{nL} [11].

$$R_n = R_{ns} - R_{nL} \text{ and} \quad (II.5)$$

$$R_n = R_{s\downarrow} - R_{s\uparrow} + R_{L\downarrow} - R_{L\uparrow} \quad (II.6)$$

Where R_{ns} is the net shortwave solar radiation, estimated by

$$R_{ns} = R_{s\downarrow} - R_{s\uparrow} = R_{s\downarrow} - \alpha R_{s\downarrow} = (1 - \alpha) R_{s\downarrow} \quad (II.7)$$

Where

$R_{s\downarrow}$: is the surface incident solar radiation (direct and diffuse) W/m^2 . Is a variable quantity, depending on several parameters (date, time, geographical position, cloudiness, etc.) and

$R_{s\uparrow} = \alpha R_{s\downarrow}$: the surface reflected solar radiation (short wave) W/m^2 and α is the **albedo** at the surface [12]

$$R_n = (1 - \alpha) R_{s\downarrow} + R_{L\downarrow} - R_{L\uparrow} \quad (II.8)$$

$R_{L\downarrow}$: atmospheric downward longwave radiation W/m^2 is depending on cloud formation.

$$R_{L\downarrow} = \varepsilon_{atm} \sigma T_{air}^4 (1 + 0.17 C_{cloud}^2) \quad [\text{Imberger and Patterson 1981}] \quad (II.9)$$

$\sigma = 5.67 \times 10^{-8} \quad W/m^2 K^4$ Boltzman constante

C_{cloud} : The fraction cloud cover coefficient ($C_{cloud}=0$ for clear sky and $C_{cloud}=1$ for totally overcast) [13]

ϵ_{atm} : the emissivity of the atmosphere (non dimensional) [14].

$$\epsilon_{atm} = 1.24 \times (e_a/T_a)^{1/7} \quad [\text{Brutsaert 1975}] \quad (\text{II.10})$$

Where

e_a Is Water Vapor Pressure in hpa and T_a is Air Temperature at **2 m Height** (Unit: K).

TABLE:II.2. Basic Empirical Methods to Estimate Atmospheric Emissivity [14]

Reference	Model
Angstrom [1924]	$\epsilon_{atm} = 0.83 - 0.18 \times 10^{-0.067.e_a}$
Brunt [1932]	$\epsilon_{atm} = 0.605 + 0.048 \times e_a^{0.5}$
Brutsaert [1975]	$\epsilon_{atm} = 1.24 \times (e_a/T_a)^{1/7}$
Idso and Jackson [1969]	$\epsilon_{atm} = 1 - 0.261 \exp(0.00077 \times (273 - T_a)^2)$
Idso [1981]	$\epsilon_{atm} = 0.7 + 5.95 \times 10^{-5} \times e_a \times \exp(1500/T_a)$
Prata [1996]	$\epsilon_{atm} = 1 - (1 + w) \times \exp(-(1.2 + 3w)^{0.5})$ $w = 46.5 \times e_a/T_a$

$R_{L\uparrow}$: the surface emitted longwave radiation W/m^2

$$R_{L\uparrow} = \epsilon_{sol} \sigma T_{soil}^4 \quad (\text{II.11})$$

ϵ_{sol} :emissivity of the soil (non dimensional).[13]

II.6.2.Sensible heat flux H:

The Sensible heat flux is a results from the transfer of convective flow of heat in the air due to the difference in temperature between the ground and the air, this heat is transported by the movement of the fluid, generated by the difference in density (natural convection), or the movement forced by the wind (forced convection)

The surface sensible heat flux calculated as follows:

$$H = h_{\text{conv}}(T_{\text{soil}} - T_{\text{air}}) \quad (\text{II.12})$$

Where h_{conv} = coefficient convective transfer coefficient estimated by the relation .

$$h_{\text{conv}} = 0,5 + 1,2\sqrt{V_{\text{wind}}} \quad (\text{II.14})$$

where: V_{wind} = Wind speed [15].

II.6.3.Latent heat flux L_vE:

Convective flow of water vapor is mass transfer, also called evapotranspiration. A transfer of latent heat accompanies this transfer. It is composed of an evaporation flow between the surface and the atmosphere, and a plant transpiration flow between the deep soil and the atmosphere. **(Neglected)**.

II.6.3.a.Evaporation - condensation

In order to satisfy the demand for water vapor from the atmosphere when it is not saturated, the water located in the ground or on the surface of the various modes of ground cover evaporates into the air. As long as the partial water vapor pressure of the air does not correspond to saturation.

Conversely, if the partial pressure of water vapor in the air is greater than the saturation vapor pressure then the water vapor condenses at the level of the surfaces or at the level of the particles present in the atmosphere [16].

Stefan's relation based on mass transfer theory also called film theory given by calculates latent heat flux can:

$$L_v E = \frac{L_v \cdot K_E \cdot M_W}{R \cdot T_a} (P_{VS}(T_S) - P_V(T_a)) \quad (II.15)$$

Where:

L_v : Latent heat of vaporization of water (J/kg)

E : Mass flux of water vapor (kg/s. m²)

K_E : Mass transfer coefficient.. (m/s)

M_W : Molar mass of water vapor (kg/mol)

R : Ideal gas constant (J/mol.K)

P_{VS} = Saturating vapor pressure given by:

$$P_{VS}(T_S) = e^{25,5058 - \frac{5204,9}{T_S}} \quad (II.16)$$

P_V = vapor pressure given by:

$$P_V(T_a) = RH P_{VS}(T_a) \quad (II.17)$$

Where **RH** : Relative humidity.

By replacing each of these quantities of the fluxes in the energy balance equation (1), we can finally write the conduction heat flux imposed as a boundary condition through the surface of the ground considered. [15]

$$G = (1 - \alpha)R_s - (\epsilon_{soil}\sigma T_{soil}^4 - \epsilon_{atm}\sigma(1 + 0.17C_{cloud}^2) T_{air}^4) + h_c \cdot (T_{air} - T_{soil}) - L_v E \quad (II.18)$$

Conclusion:

In this chapter, we have provided a general overview of heat transfer within soil and its different mechanism. In addition, their mathematical equation that help us to put module of this physic phenomena in order to represent the surface energy balance, that control soil surface temperature.

References:

- [1] [Heat Transfer \(gsu.edu\)](#) 20/05/2022
- [2] RAJPUT, R.K. *Heat and mass transfer*. ram nagar, new delhy. S shanda and company ltd.2000.
- [3] **Incropera, F. P., & DeWitt, D. P.** *Fundamentals of heat and mass transfer*. New York: J. Wiley. (2002).
- [4] [What Is Convection? - Heat Definition, Types of Convection, Examples, Video and FAQs \(byjus.com\)](#) 20/05/2021
- [5] [thermal radiation | Definition, Properties, Examples, & Facts | Britannica](#) 21/05/2022
- [6] [Longwave and Shortwave Radiation | North Carolina Climate Office \(ncsu.edu\)](#) 15/05/2022
- [7] [13.2 Soil Thermal Properties – Rain or Shine \(okstate.edu\)](#) 12/05/2022
- [8] [Longwave and Shortwave Radiation | North Carolina Climate Office \(ncsu.edu\)](#) 15/05/2022
- [9] [Shortwave Radiation \(army.mil\)](#) 15/05/2022
- [10] [Surface Heat Flux Parameterization and Surface Energy Balance | DR. YI DENG \(gatech.edu\)](#) 15/05/2022
- [11] **Lincoln Zotarelli et al** , *Step by Step Calculation of the Penman-Monteith Evapotranspiration (FAO-56 Method)* , University Edition, University of Florida IFAS, 2020
- [12] Bezerra, B.G., da Silva, B.B., dos Santos, C.A.C. and Bezerra, J.R.C. (2015) Actual Evapotranspiration Estimation Using Remote Sensing: Comparison of SEBAL and SSEB Approaches. *Advances in Remote Sensing*, 4, 234-247.
- [13] **Sedighi, M., Hepburn, B. D., Thomas, H. R., & Vardon, P. J.** (2016). Energy balance at the soil atmospheric interface. *Environmental Geotechnics*, 5(3), 146-157.
- [14] D. Guo et al.: Sensitivity of potential evapotranspiration to changes in climate variables s for different Australian climatic zones.
- [15] **MABROUKI, D.** . *Étude de l'influence des paramètres climatiques sur la température du sol (application au site de Biskra)* ,Biskra university,(Master's thesis) 2014.
- [16] **DUPONT S,***modelisation dynamique et thermodynamique de la canopee urbaine : realisation du modele de sols urbains pour submeso*,university of nantes, doctoral thesis,(2001)

Chapter III

*Mathematical Modeling and
Numerical Simulation*

III.1.Introduction

To estimate the variation of soil surface temperature we must solve the energy balance equation that we extracted on the precedent chapter. in this chapter we present the method (FVM) and the different parameters that aide us step by step.

III.2.General principles of the finite volume method

The finite volume method (FVM) is a discretization method well adapted to the numerical resolution of the conservation equations of extensive quantities such as mass, quantity of motion, energy. .This method has various properties such as the local conservation of flows, the respect of the principle of maximum, the possibility of applying it to any meshes (structured or unstructured meshes) that make it attractive. Another advantage of this method is that it leads four robust numerical scheme. This explains why this method is widely used in various fields: fluid mechanics, heat and mass transfer, reservoir simulation in petroleum engineering. The finite volume method is based on an integral formulation of the continuous problem, which has been treated [1].

III.3.Equation of the problem:

The mathematical formulation of this problem based on the conduction equation, which together with the boundary conditions and at the ground-air interface solved by the finite volume method. According to the hypotheses considered:

Consider unsteady flow on **2D** dimension **x,y axis** ,convection term neglected and the soil without heat source so source term **S=0**.

The equation of thermal conduction in the soil considered two-dimensional is of the form as follows:

$$\rho C_p \frac{\partial T}{\partial t} = \frac{\partial}{\partial x} \left(\lambda \frac{\partial T}{\partial x} \right) + \frac{\partial}{\partial y} \left(\lambda \frac{\partial T}{\partial y} \right) \quad \text{(III.1)}$$

ρ : Average soil density [**kg/m³**]

C_p : Average mass heat capacity of soil [**J/kg K**]

λ : Average thermal conductivity of soil [**W/m K**]

T: Temperature [**K**] at a point on the ground identified by the coordinates (x,y,z) and at the instant **t** [**s**].

(**x, y, z**) : Spatial coordinates of the considered point in the ground [**m**]

The flow **G** is the net flow absorbed and conducted throughout the ground and subsoil domain that we can consider as a semi-infinite massif represented by the following figure:

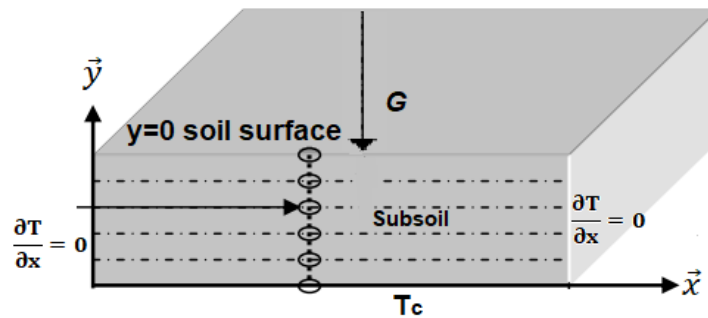


Figure.III.1 Soil modeling

III.4.The boundary conditions.

The calculation domain schematized by the figure represents the various boundary conditions considered and are as follows:

III.4.a.Boundary conditions on the top face (soil surface):

The conduction heat flux **G** soil surface resulting from the energy balance equation.

We can consider that the exchange flow is only on the **Y-axis**

III.4.b.Boundary conditions on the bottom face (subsoil):

We know that at a certain depth in the ground the temperature remains constant, the value of which is specific to the geographical location and the geological nature of the subsoil.

The temperature determined by experimental measurement reading at **5 meter** on the place of **Biskra** considered as **Tc=17C°**.

Then we must impose on this depth a constant temperature **Tc= 17C°** as a condition at the boundary of the domain.

III.4.c. Boundary condition on the frontier (right left)

The domain is considered as semi-infinite then on the frontier in the direction of the **x**-axis we can consider that the exchange flow is zero $\frac{\partial T}{\partial x} = 0$

III.5. Domain discretization:

Using the FVM, the domain is divided into discrete control volumes defined by nodal points. These nodal points define the space between boundary conditions as described in **Figure.III.1**.

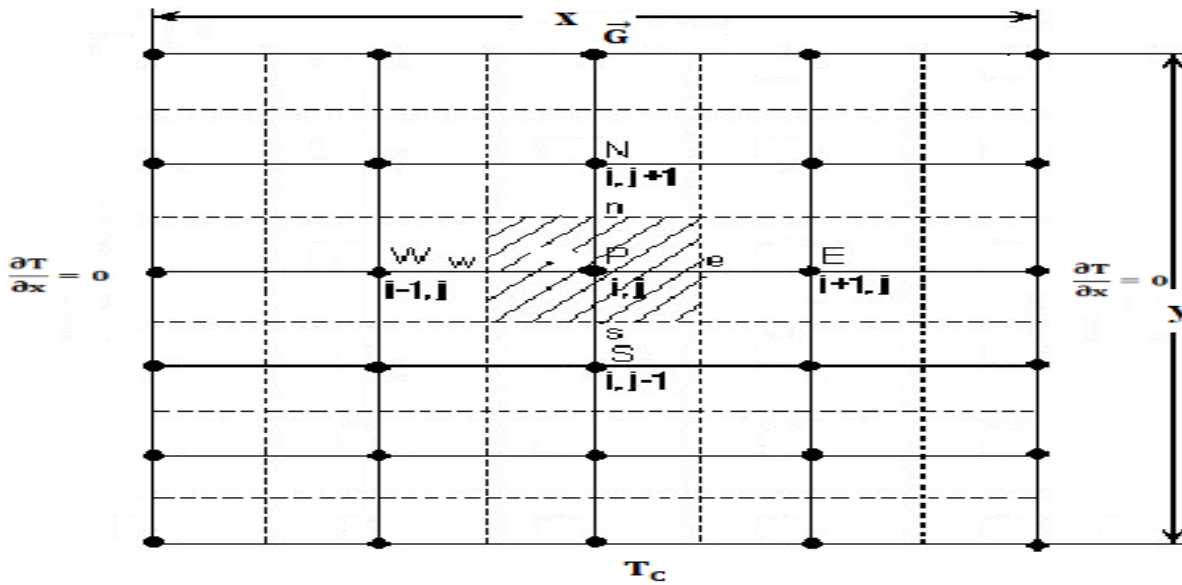


Figure.III.2. calculation mesh [2]

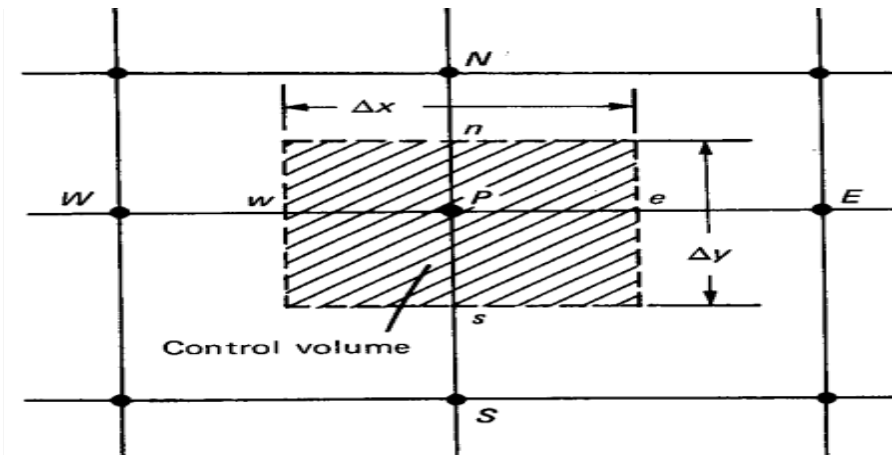


Figure.III.3. Control volume [3]

III.6. Discretization of the equation [5]:

By the integration of equation (III.1) on the control volume (**Figure.III.3**) and on the time from **t** to **t+Δt** then we finde:

$$\int_t^{t+\Delta t} \int_{VC} \rho C_p \frac{\partial T}{\partial t} dV dt = \int_t^{t+\Delta t} \int_{VC} \frac{\partial}{\partial x} \left(\lambda \frac{\partial T}{\partial x} \right) dV dt + \int_t^{t+\Delta t} \int_{VC} \frac{\partial}{\partial y} \left(\lambda \frac{\partial T}{\partial y} \right) dV dt \quad (III.2)$$

$$\rho C_p (T_P - T_P^0) \Delta x \Delta y = \int_t^{t+\Delta t} \left(\lambda_e \left(\frac{\partial T}{\partial x} \right)_e - \lambda_w \left(\frac{\partial T}{\partial x} \right)_w \right) \Delta y dt + \int_t^{t+\Delta t} \left(\lambda_n \left(\frac{\partial T}{\partial x} \right)_n - \lambda_s \left(\frac{\partial T}{\partial x} \right)_s \right) \Delta x dt \quad (III.3)$$

By replacing the temperature gradients, we get:

$$\rho C_p (T_P - T_P^0) \Delta x \Delta y = \int_t^{t+\Delta t} \left(\lambda_e \left(\frac{T_E - T_P}{\delta x_e} \right) - \lambda_w \left(\frac{T_P - T_W}{\delta x_w} \right) \right) \Delta y dt + \int_t^{t+\Delta t} \left(\lambda_n \left(\frac{T_N - T_P}{\delta n} \right) - \lambda_s \left(\frac{T_P - T_S}{\delta x_s} \right) \right) \Delta x dt \quad (III.4)$$

By using the **fully implicit scheme**, then we obtain the equation:

$$\rho C_p (T_P - T_P^0) \frac{\Delta x \Delta y}{\Delta t} = \lambda_e \left(\frac{T_E - T_P}{\delta x_e} \right) \Delta y - \lambda_w \left(\frac{T_P - T_W}{\delta x_w} \right) \Delta y + \lambda_n \left(\frac{T_N - T_P}{\delta y_n} \right) \Delta x - \lambda_s \left(\frac{T_P - T_S}{\delta y_s} \right) \Delta x \quad (III.5)$$

By assembling the terms we obtain the general form of the discretized equation:

$$\mathbf{a}_p T_P = \mathbf{a}_w T_W + \mathbf{a}_E T_E + \mathbf{a}_S T_S + \mathbf{a}_N T_N + \mathbf{b} \quad (III.6.1)$$

Where

$$\mathbf{a}_w = \frac{\lambda_w A_w}{\delta x_w} \quad (III. 6.1) \quad \mathbf{a}_E = \frac{\lambda_e A_e}{\delta x_e} \quad (III. 6.2)$$

$$\mathbf{a}_S = \frac{\lambda_s A_s}{\delta y_s} \quad (III. 6.3) \quad \mathbf{a}_N = \frac{\lambda_n A_n}{\delta y_n} \quad (III. 6.4)$$

With

$$\mathbf{a}_p = \mathbf{a}_w + \mathbf{a}_E + \mathbf{a}_S + \mathbf{a}_N + \mathbf{a}_p^0 \quad (III. 7)$$

$$\mathbf{a}_p^0 = \rho C_p \frac{\Delta x \Delta y}{\Delta t} \quad (III. 7.1) \quad \text{and} \quad \mathbf{b} = \mathbf{a}_p^0 T_P^0 \quad (III. 7.2)$$

III.7.Solution of Algebraic Equations:

After discretization on each volume control, we find a system of algebraic equation. Which fills a sparse matrix that can easily solved by an iterative method is required. The Thomas algorithm, or tri-diagonal matrix algorithm (TDMA), is a commonly used line-by-line solver that is computationally inexpensive and has minimal storage requirements. In the present work, the TDMA methods is implemented in MATLAB

III.7.1. Thomas algorithm or the TDMA (TriDiagonal-Matrix Algorithem)

The Algorithm of Tri-Diagonal Matrix (TDMA), also known under the name of **Thomas algorithm**, is a simplified form of Gaussian elimination, which can used to solve the system of equations with three diagonal. **TDMA** based on Gaussian elimination procedure and consist of two parts - a forward elimination phase and a backward substitution phase. **TDMA** is in fact a direct method, but can applied iteratively in a line-by-line fashion, to solve multidimensional problems and is widely used in **CFD** programs.

To solve the above **TDMA** system along **North-South** lines, the discrete equation (III.7) reorganized in the form

$$\mathbf{a}_i \mathbf{T}_i = \mathbf{b}_i \mathbf{T}_{i+1} + \mathbf{c}_i \mathbf{T}_{i-1} + \mathbf{d}_i \quad \text{where} \quad \mathbf{1} \leq \mathbf{i} \leq \mathbf{N} \quad (\text{III.8})$$

The temperature \mathbf{T}_i is expressed as a function of the neighboring temperatures \mathbf{T}_{i-1} and \mathbf{T}_{i+1} . To take into account the special form of the equations for the boundary points (**1**) and (**N**) it is necessary that:

$$\mathbf{c}_1 = \mathbf{0} \quad \text{and} \quad \mathbf{b}_N = \mathbf{0}. \quad (\text{III.9})$$

for ($\mathbf{i} = \mathbf{1}$), the temperature \mathbf{T}_1 is known we have $\mathbf{a}_1 = \mathbf{0}$, $\mathbf{b}_1 = \mathbf{0}$, $\mathbf{c}_1 = \mathbf{0}$ et $\mathbf{d}_1 = \mathbf{T}_1$.

In the equation (7) for ($\mathbf{i}=2$), is a relationship between \mathbf{T}_1 , \mathbf{T}_2 et \mathbf{T}_3 , in fact \mathbf{T}_1 is expressed as a function of known \mathbf{T}_2 , the relationship between \mathbf{T}_1 , \mathbf{T}_2 and \mathbf{T}_3 ,is reduced to a relationship between \mathbf{T}_2 and \mathbf{T}_3 , i.e. \mathbf{T}_2 can be expressed as a function of \mathbf{T}_3 .

The substitution process continues until \mathbf{T}_N which is expressed as a function of \mathbf{T}_{N+1} which plays no role since ($\mathbf{b}_N = \mathbf{0}$), so we obtain, in this step, the value of \mathbf{T}_N .

We then start the inverse process where we determine \mathbf{T}_{N-1} according to \mathbf{T}_N , \mathbf{T}_{N-2} according to \mathbf{T}_{N-1} and so on until \mathbf{T}_2 written according to \mathbf{T}_3 while \mathbf{T}_1 is a function of \mathbf{T}_2 . The substitution process continues forward according to the steps as follows:

$$\mathbf{a}_1 \mathbf{T}_1 = \mathbf{b}_1 \mathbf{T}_2 + \mathbf{0} + \mathbf{d}_1 \rightarrow \mathbf{T}_1 = \mathbf{f}(\mathbf{T}_2) = \frac{\mathbf{b}_1}{\mathbf{a}_1} \mathbf{T}_2 + \frac{\mathbf{d}_1}{\mathbf{a}_1} \quad (\text{III.10})$$

$$\mathbf{a}_2 \mathbf{T}_2 = \mathbf{b}_2 \mathbf{T}_3 + \mathbf{c}_2 \mathbf{T}_1 + \mathbf{d}_2 \rightarrow \mathbf{T}_2 = \mathbf{f}(\mathbf{T}_3) \quad (\text{III.11})$$

$$\mathbf{a}_3 \mathbf{T}_3 = \mathbf{b}_3 \mathbf{T}_4 + \mathbf{c}_3 \mathbf{T}_2 + \mathbf{d}_3 \rightarrow \mathbf{T}_3 = \mathbf{f}(\mathbf{T}_4) \quad (\text{III.12})$$

$$\mathbf{a}_{N-1} \mathbf{T}_{N-1} = \mathbf{b}_{N-1} \mathbf{T}_N + \mathbf{c}_{N-1} \mathbf{T}_{N-2} + \mathbf{d}_{N-1} \rightarrow \mathbf{T}_{N-1} = \mathbf{f}(\mathbf{T}_N) \quad (\text{III.13})$$

$$\mathbf{a}_N \mathbf{T}_N = \mathbf{0} + \mathbf{c}_N \mathbf{T}_{N-1} + \mathbf{d}_N \rightarrow \mathbf{T}_N = \mathbf{Q}_N \quad (\text{III.14})$$

In this step, we are looking for relations of the type $\mathbf{T}_i = \mathbf{f}(\mathbf{T}_{i+1})$ in the form

$$\mathbf{T}_i = \mathbf{P}_i \mathbf{T}_{i+1} + \mathbf{Q}_i \quad (\text{III.15})$$

but we can also write the following relation:

$$\mathbf{T}_{i-1} = \mathbf{P}_{i-1} \mathbf{T}_{i+1} + \mathbf{Q}_{i-1} \quad (\text{III.16})$$

By replacing equation (III.16) in equation (III.8) we obtain:

$$\mathbf{a}_i \mathbf{T}_i = \mathbf{b}_i \mathbf{T}_{i+1} + \mathbf{c}_i \mathbf{T}_{i-1} + \mathbf{d}_i \quad (\text{III.17})$$

$$\mathbf{a}_i \mathbf{T}_i = \mathbf{b}_i \mathbf{T}_{i+1} + \mathbf{c}_i \mathbf{T}_{i-1} (\mathbf{P}_{i-1} \mathbf{T}_i + \mathbf{Q}_{i-1}) + \mathbf{d}_i \quad (\text{III.18})$$

En regroupant les termes dans l'équation (III.18) sous la forme générale (III.16) on obtient les coefficients \mathbf{P}_i et \mathbf{Q}_i en fonction des coefficients \mathbf{P}_{i-1} et \mathbf{Q}_{i-1} :

By grouping the terms in equation (III.18) in the general form (III.16) we obtain the coefficients \mathbf{P}_i and \mathbf{Q}_i as a function of the coefficients \mathbf{P}_{i-1} and \mathbf{Q}_{i-1} :

$$\mathbf{P}_i = \frac{\mathbf{b}_i}{\mathbf{a}_i - \mathbf{c}_i \mathbf{P}_{i-1}} \quad (\text{III.19})$$

$$\mathbf{Q}_i = \frac{\mathbf{d}_i + \mathbf{c}_i \mathbf{Q}_{i-1}}{\mathbf{a}_i - \mathbf{c}_i \mathbf{P}_{i-1}} \quad (\text{III.20})$$

To start the recurrence process we note that for $i=1$ the equation (III.8) is already in the form (III.15) and the values of P_1 et Q_1 are given by the following formulas:

$$P_1 = \frac{b_1}{a_1} \quad \text{and} \quad Q_1 = \frac{d_1}{a_1} \quad (\text{III.21})$$

It is good to specify that the relations (III.21) are obtained if we replace $c_1 = 0$ in the relations (III.19) and (III.20). At the end of the recurrence process we find that $b_N = 0$ and therefore $P_N = 0$ and from equation (III.15) we obtain:

$$T_N = Q_N \quad (\text{III.22})$$

At this point, we are in the situation to start the backward substitution process using the relation (III.15) [4].

III.7.2. Summary of the algorithm

1. Calculate P_1 and Q_1 using the relations (III.21)
2. Calculate P_i and Q_i , for $i = 2 \div N$, with the recurrence relations (III.19) and (III.20).
3. Put $T_N = Q_N$.
4. Use the equation $T_i = P_i T_{i+1} + Q_i$ for varying from $i = N - 1$ to 1 to obtain

$$T_{N-1}, T_{N-2}, \dots, T_1. \quad [3]$$

III.8.Simulation part:

To simulate the behavior of the ground subjected to the climatic conditions of Biskra, we are based on the meteorological data collected at the level of the local station of Biskra in 2005.to used it as input data in **MATLAB** code that we would like to program.

III.8.1.Station description:

Biskra is a city located in north of the Algerian Sahara ($34^\circ 51' 01''$ Nord , $5^\circ 43' 40''$ Est) with an elevation of **115 m** [5] , in the foothills of the Aures and Zab Mountains, 400 km south-east of Algiers, capital of Algeria. Biskra Climate is sropical and subtropical desert [6]

At Biskra region , the soil is characterized as sandy loam soil texture [**0cm - 60 cm**], loamy sand [**20 cm - 60 cm**] and clayey sand beyond **60 cm** [7] .

The surface parameters and soil parameters in this simulation are listed in **Table 2**

Table. III.1: The proprieties of the soil in the region of Biskra[7]

Soil proprieties	Value
Specific heat	1340 j.K⁻¹.Kg⁻¹
Thermal conductivity	1.5 W.K⁻¹m⁻¹
Surface Emissivity	0.73
Density	1800 Kg^m⁻³
Albedo	0.35

III.8.2. Meteorological data

The meteorological data collected at the level of the local metrological station of Biskra in 2005. We used the average values of global radiation, ambient temperature, wind speed, and relative humidity, in hourly evolution, recorded for typical days for the twelve months of the year. The table below summarizes this data.

Table. III.2: Annual meteorological data of the ambient (metrological station of Biskra2005)[8].

Month	Global radiation W/m2	Temperature T° moy °C	Wind Speed V m/s	Relative humidity of the air HR moy %
January	221	10	04.6	53
February	232	10.7	03.9	51
March	270	17.8	04.2	41
April	298	21.8	05.3	32
May	320	27.9	03.7	28
June	358	31.7	04	29
July	371	35.9	03.5	26
August	334	27.2	03.4	29
September	268	28.5	03.5	46
October	251	24	02.1	51
November	215	17.7	03.7	54
December	219	10.8	03.1	66

III.8.3 Calculating Algorithms

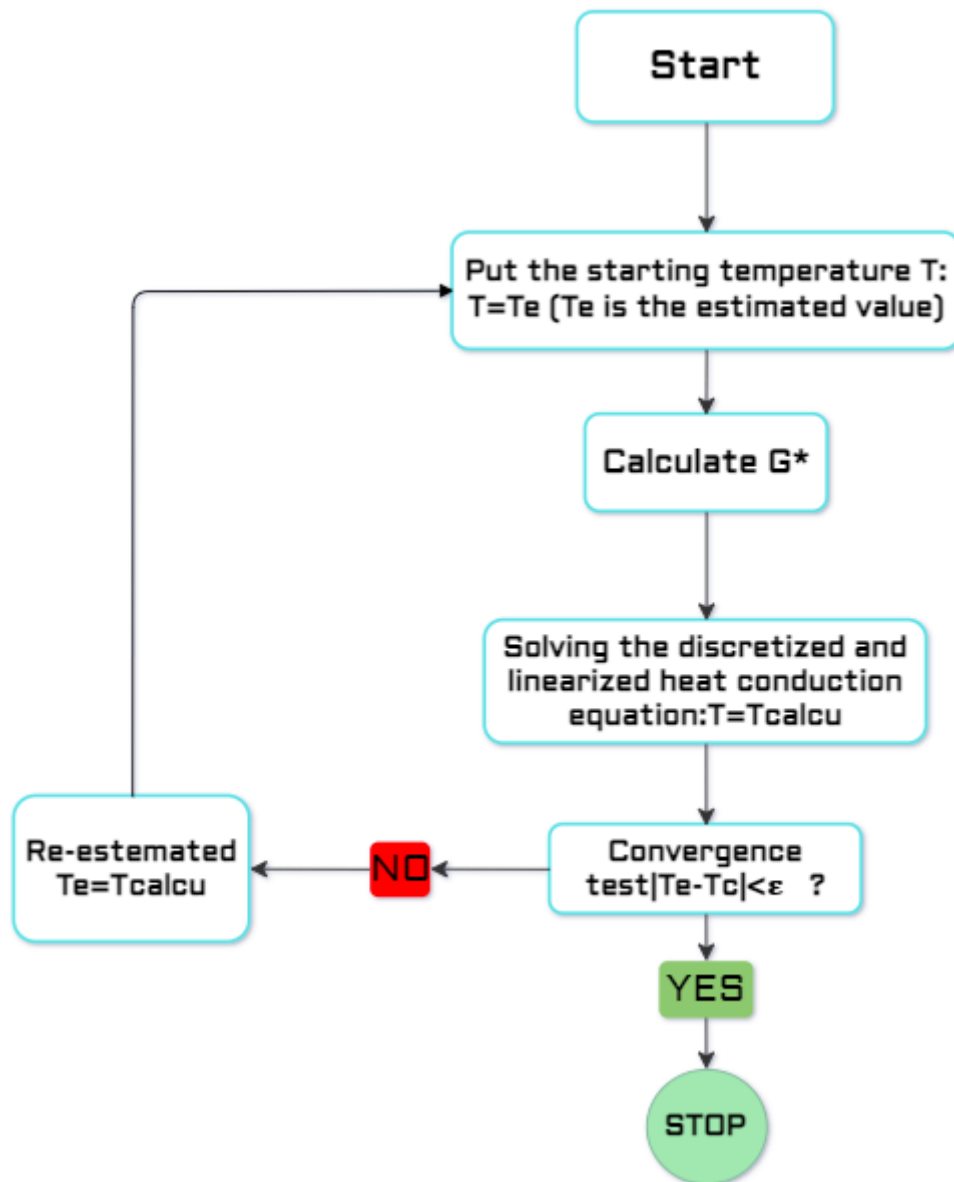


Figure.III.1: Algorithm for calculating surface temperature for an average monthly day

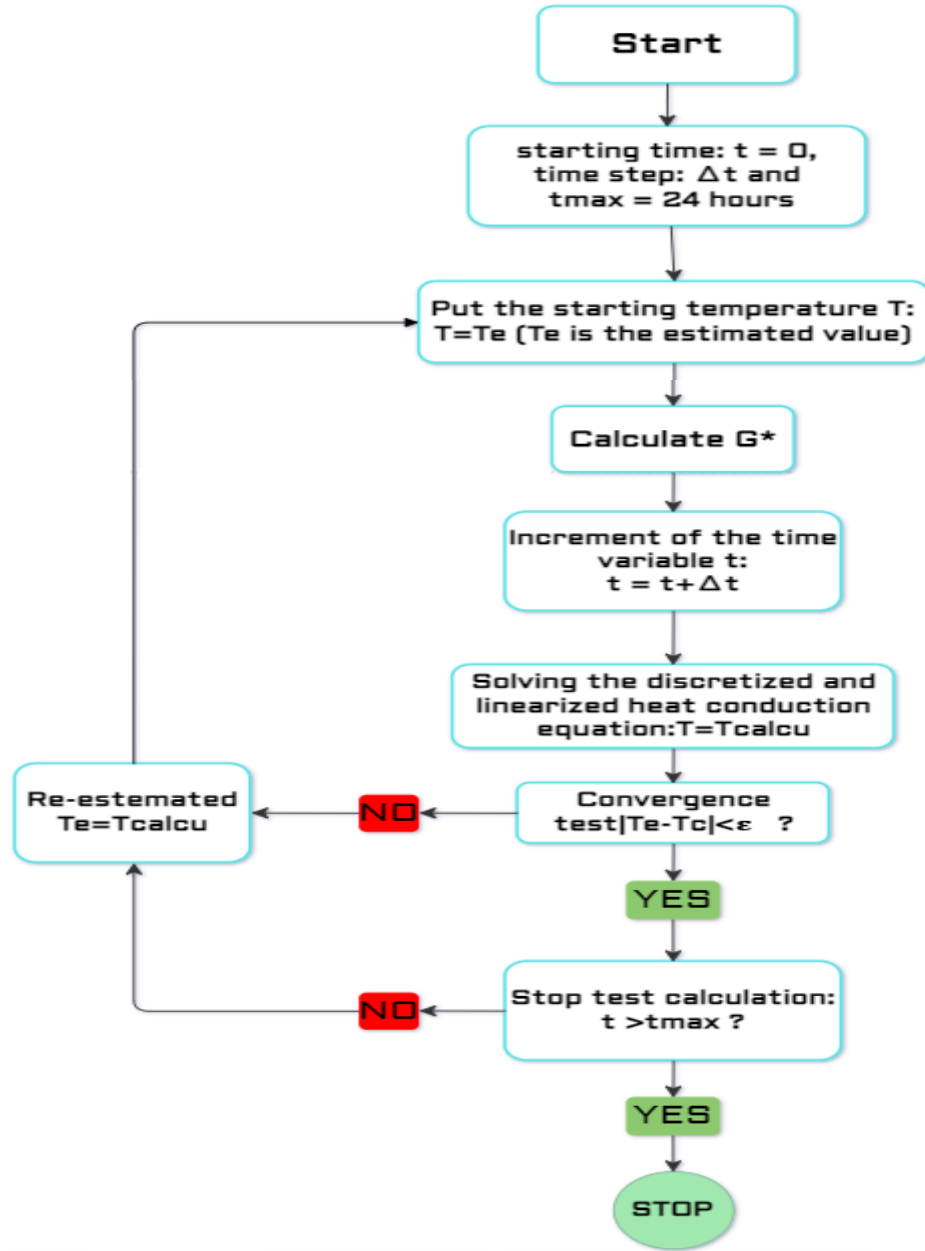


Figure.III.2: Algorithm for calculating surface temperature for 24 hours

III.9.Conclusion

We presented the solution method, meteorological data and the algorithms that help us to coding Matlab program that find the variation of the soil surface temperature.

References

[1]BELKAID.N.Simulation numérique des transferts thermique et massique dans un sol non sature.Tizi-ouzou university.2011

[2]ARBI,A. Etude de la conduction de la chaleur, application de la méthode de volumes finis à la conduction thermique dans le sol (Master's theme).Biskra university (2019).

[3]S. V. Patankar, Numerical heat transfer and fluid flow. Mc Graw –Hill, New York (1980).

[4]Popa I. C., Modélisation numérique du transfert thermique. Méthode des volumes finis, University Edition, Craiova, 2002.

[5][Les coordonnées géographiques de Biskra. La latitude, la longitude et l'altitude par rapport au niveau de la mer de Biskra, Algérie \(dateandtime.info\) 01/06/2022](#)

[6]Kotték, M., Grieser, J., Beck, C., Rudolf, B., & Rubel, F. World map of the Köppen-Geiger climate classification updated. (2006).

[7]MABROUKI, D. . *Étude de l'influence des paramètres climatiques sur la température du sol (application au site de Biskra)* ,Biskra university,(Master's thesis) 2013.

[8] A. Ben Aziza et H. Lebed “caractérisation de quelques variétés d’abricotiers dans la région de M’chouneche Wilaya de Biskra” courrier du savoir N°08, Biskra university , 2007 pp 101-110.

Chapter IV

Result

And Discussion

IV.1.Introduction:

In order to determine the influence of a large number of environmental parameters as the ambient temperature and the wind speed ... etc, essentially on the soil surface of the ground, we took a typical day for each months, (a monthly average is taken for each month of the year).

IV.2.a. Effect of solar radiation:

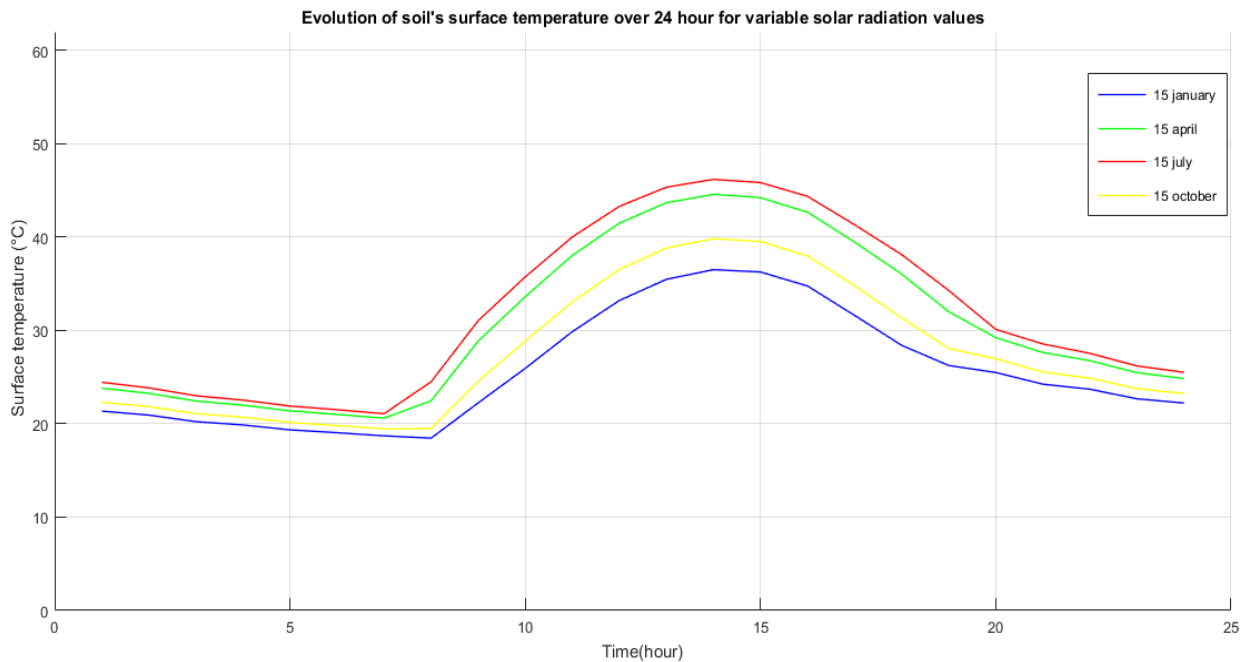


Figure IV.1: Evolution of surface temperature for different solar radiation values over 24h.

- ❖ The (Figure.IV.1) shows the developments of the ground surface temperature with each change in the value of solar radiation, we note that when solar radiation flux increase, the temperature of the soil surface augment.
- ❖ The maximum difference between the curves at the different values is located in the middle of the day equal to 9 C

IV.2.b. Effect of ambient temperature

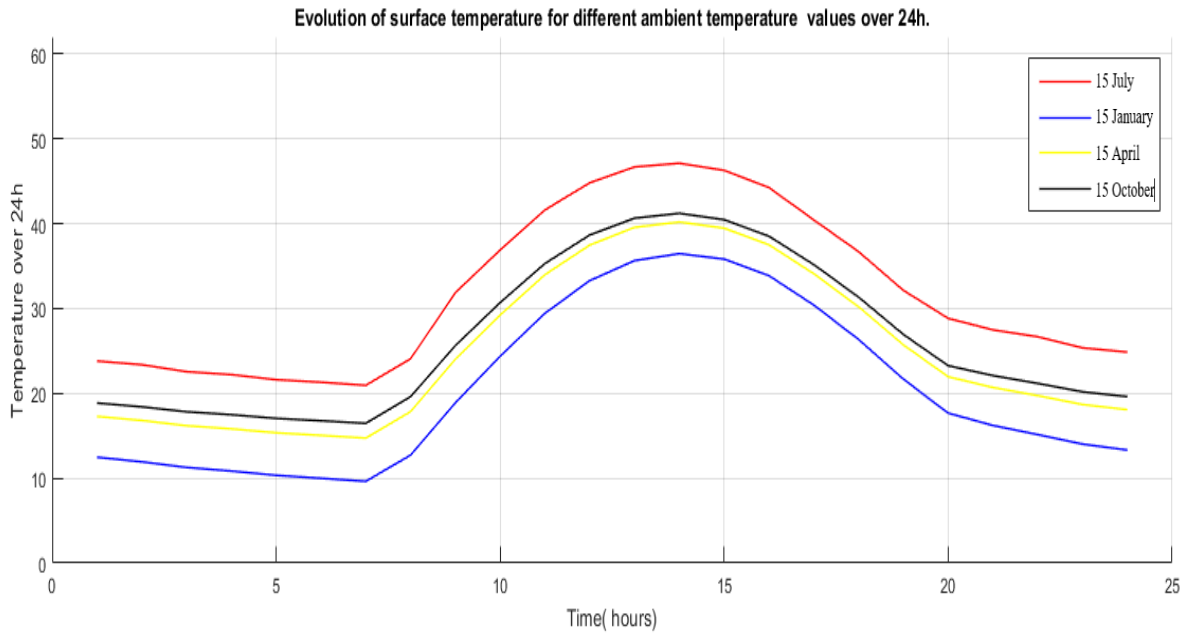


Figure .IV.2: Evolution of surface temperature for different ambient temperature values over 24h.

- ❖ The (Figure.IV.2) shows the developments of the ground surface temperature with each change in the value of ambient temperature, we note that when ambient temperature augment the temperature of the soil surface augment and vice versa.
- ❖ The maximum difference between the curves at the different values is located in the middle of the day equal to 12 C

IV.2.c.Effect of wind speed:

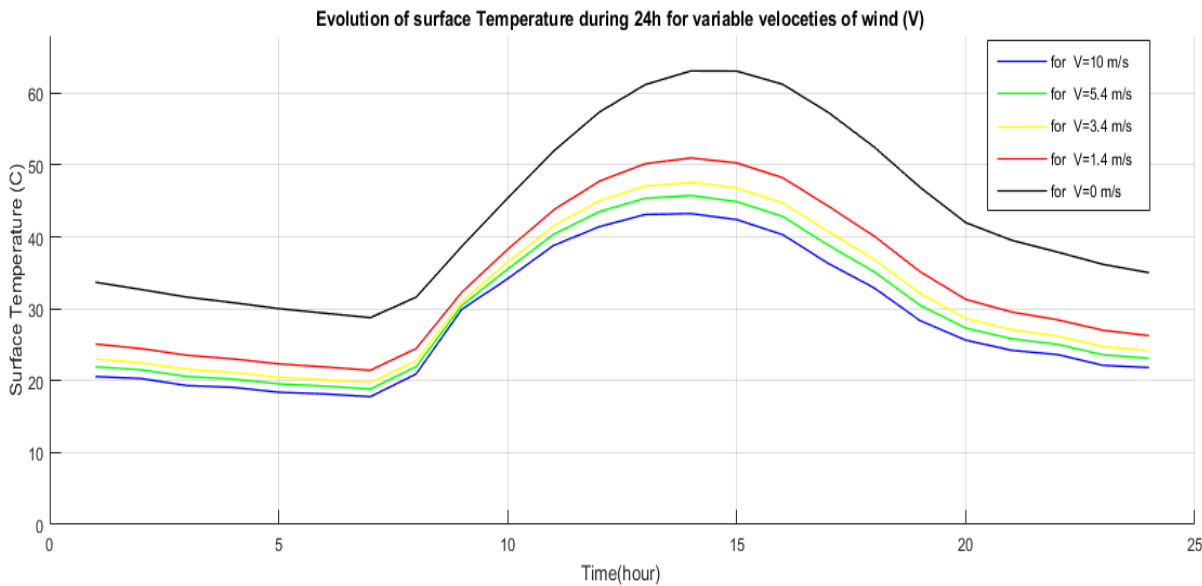


Figure.IV.3.Evolution of surface temperature for different wind speed values over 24h.

- ❖ The (Figure.IV.3) shows the developments of the ground surface temperature with each change in the wind speed value, we note that when the wind speed increases the temperature on the ground decreases, because when the wind accelerates, the value of convective heat transfer coefficient increases, This heat exchange between the ground surface and the air so sensible heat flux increases, and the ground cools rapidly. **Also because** the acceleration of the wind make the evaporation process done a lot.
- ❖ The maximum difference between the curves at the different values is located in the middle of the day equal to 20 C

IV.2.d.Effect of relative humidity:

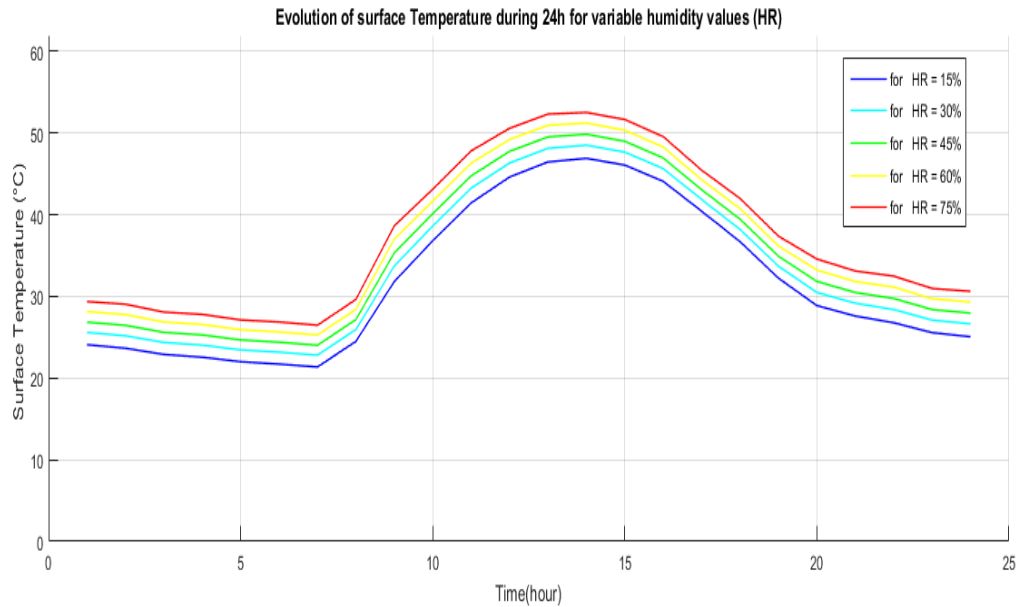


Figure.IV.4: Evolution of surface temperature for different relative humidity values over 24h.

- ❖ The (Figure.IV.4) shows the developments of the surface temperature of the ground with each change in the value of humidity, we note that when the humidity increases the temperature on the ground decreases, because when the humidity augments, the vapor pressure approaches to the saturation vapor pressure, and Thus, the ground keeps its heat and does not participate in the evaporation process as a latent heat.
- ❖ The maximum difference between the curves at the different values is located in the middle of the day equal to 6 C

IV.2.e.Effect of fractional cloud cover coefficient:

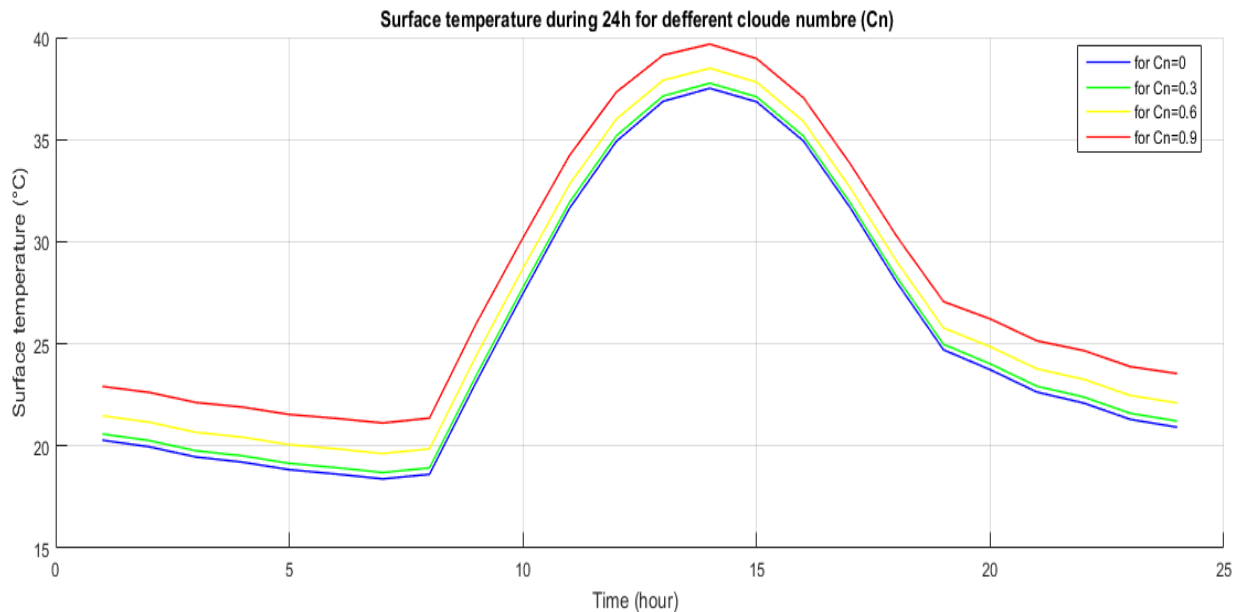


Figure .IV.5: Evolution of surface temperature for different cloud number values over 24h.

- ❖ The (Fig.IV.5) shows the developments in the surface temperature of the ground with each change in the value of the cloud cover coefficient. We notice that when the cloud cover coefficient increases, that is, the more clouds the sky is covered, the temperature on the ground increases, because these clouds trap the radiation reflected from the ground, And it reflects back to it again and again, which means that the radiation on the ground is increased. Cloudy sky act like polluting gases (CO₂, Nox, etc) in the atmosphere and their influence are similar to the greenhouse effect.
- ❖ The maximum difference between the curves at the different values is located in the middle of the day equal to 3 C

IV.2.f.Effect of surface albedo:

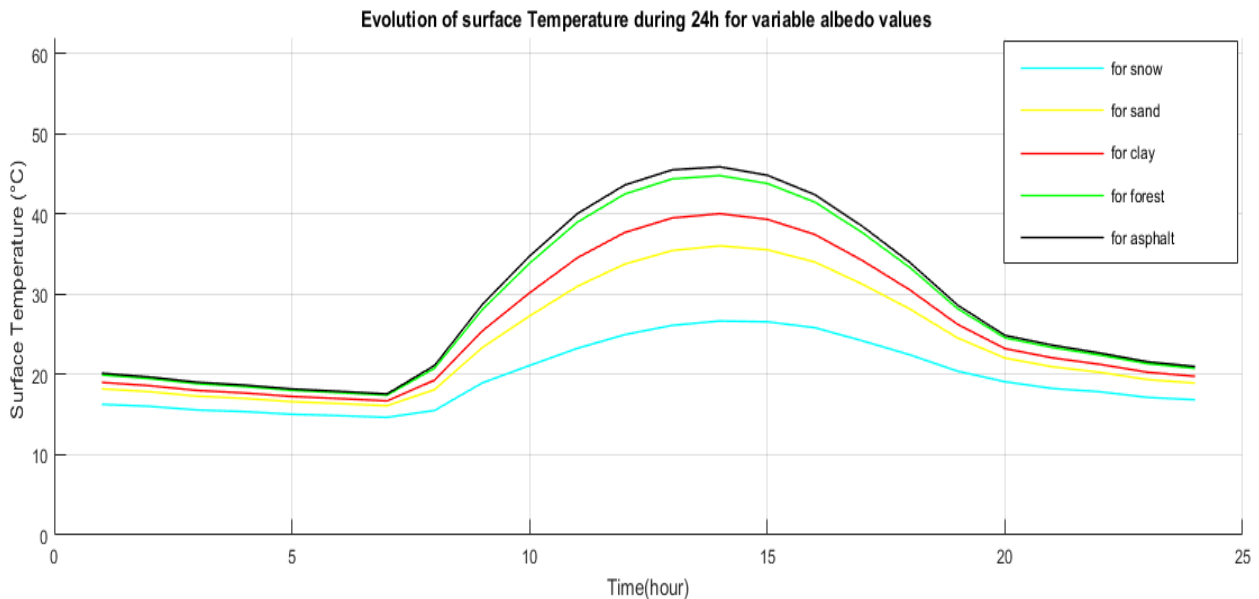


Figure.IV.6: Evolution of surface temperature for different albedo values over 24h.

- ❖ The (Figure.IV.6) shows the developments of the ground surface temperature with each change in the value of surface albedo, we note that surfaces that tend to darken like Asphalt have high temperatures, while those that tend to whiten like snow are low, because the shortwave radiation incident from the sun when it falls on white surfaces is mostly reflected and not absorbed by the ground, keeping the ground or body cold.
- ❖ This observation can be exploited as the researcher did (Shweta Sharma and al) where they studied the effect of surface Albedo change (using white paint on surfaces in India) on the change in the temperature of the ground surface. The study concluded that use of cool roofs in India could compensate the heating due to increase in CO₂ (from pre-industrial to current times) by ~ 5%.
- ❖ The maximum difference between the curves at the different values is located in the middle of the day equal to 21 C

IV.2.g. Effect of surface emissivity:

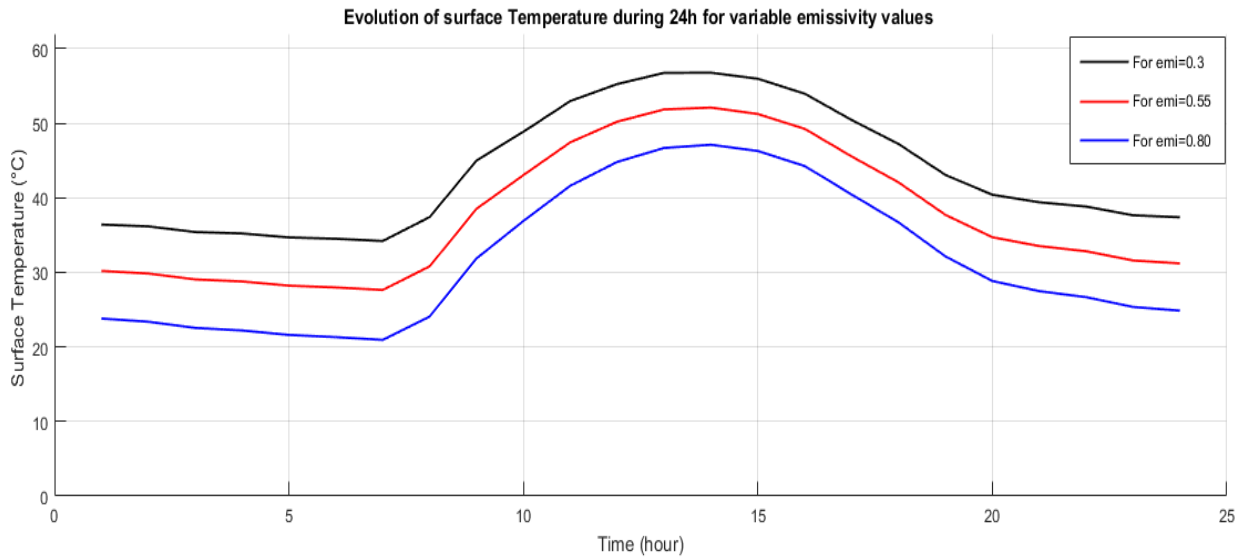


Figure .IV.7: Evolution of surface temperature for different emissivity values over 24h.

- ❖ The (Figure .IV.7) shows the developments of the ground surface temperature with each change in the value of surface emissivity. We note that the surface temperature increases with high surface emissivity value and vice versa, the surface temperature decreases with low surface emissivity value. This is because the soil or body stays could by emitting more radiation as its emittance increases.
- ❖ The temperature difference between the curves is more and more important according to the emissivity.
- ❖ The maximum difference between the curves at the different values is located in the middle of the day equal to 10 C.

Conclusion:

We presented the effect of the different environmental parameter on the soil surface temperature and we discussed them.

General conclusion:

Due to its importance of soil temperature and the severity of need and the lack of information on it, it is therefore necessary for us to interest and contribute to improving knowledge of the phenomena related to it and how the environmental factors affect the soil's surface temperature.

The soil's surface temperature depends on the energy balance on the soil's surface, as it affected by seasonal change, insolation, the absence/presence of clouds, and air temperature.

The study also proved that dark soil (albedo is close to zero) absorbs more solar radiation, so the darker its color, the faster its temperature rises, and vice versa also wind speed affects the soil surface directly by increasing the heat exchange coefficient and increasing the evaporation process. As for the effect of relative humidity on the soil surface temperature, it is inverse, as the increase in humidity decreases the soil surface temperature, which in turn prevents the evaporation process.

In this study, we found that the governing factors in soil temperature are arranged according to influence as follows: At first the Albedo and the wind speed, then solar radiation and the surface emissivity followed by the ambient temperature and relative humidity, and at last the cloud cover coefficient.

Temperature affect biological, chemical, and physical features of soil either decrease or increase them.

At last we hope that this study will follow by an experimental study to prove our results ,and utilize it on the agriculture to solve many problems as plant growth according to modify the soil temperature ,and in the geothermal engineering to improve their performance and then minimize the pollution and participate to solve the crisis of energy also in the sector of pollution and global warming through rise the surface albedo and minimize the solar radiation stocked in the soil through augment the emittance of the soil

المخلص

يهدف هذا العمل إلى دراسة تأثير العوامل المناخية والبيئية على درجة حرارة التربة. باستخدام معادلة توازن الطاقة على سطح التربة من خلال النمذجة العددية وهي طريقة الحجوم المنتهية في برنامج ماتلاب أظهرنا تطور درجة حرارة سطح التربة وكذلك كيفية تأثير العوامل البيئية المختلفة عليها. تظهر نتائج الدراسة الحالية أن العوامل المناخية لها تأثيرات متفاوتة ومهمة في خفض ورفع درجة حرارة سطح التربة.

الكلمات المفتاحية: العوامل المناخية والبيئية، معادلة توازن الطاقة، درجة حرارة سطح التربة، النمذجة العددية، برنامج ماتلاب

Abstract:

This work aim to study the influence of climatic and environmental factors on soil temperature. By using the energy balance equation on soil surface through numerical modeling which is the Finite volume method (FVM), followed by computer MATLAB code, we have shown the evolution of soil surface temperature as well as how various environmental factors affect it. The results of the current study show that climatic factors have varying and important effects in lowering and raising the temperature of the soil surface.

Keywords: climatic and environmental factors, energy balance equation, soil surface temperature, numerical modeling, MATLAB code.

Résumé:

Ce travail a pour objectif d'étudier l'influence des facteurs climatiques et environnementaux sur la température du sol. En utilisant l'équation du bilan énergétique à la surface du sol à travers la modélisation numérique qui est la Méthode des volumes finis (MVF), suivie du code informatique MATLAB, nous avons montré l'évolution de la température de surface du sol ainsi que la façon dont divers facteurs environnementaux l'affectent. Les résultats de l'étude actuelle montrent que les facteurs climatiques ont des effets variables et importants sur l'abaissement et l'élévation de la température de la surface du sol.

Mots clés : facteurs climatiques et environnementaux, équation du bilan énergétique, température de surface du sol, modélisation numérique, code MATLAB.